

Accepted Manuscript

Discovery of potent azaindazole leucine-rich repeat kinase 2 (LRRK2) inhibitors possessing a key intramolecular hydrogen bond — Part 2

Daniel G.M. Shore, Zachary K. Sweeney, Alan Beresford, Bryan K. Chan, Huifen Chen, Jason Drummond, Andrew Gill, Tracy Kleinheinz, Xingrong Liu, Andrew D. Medhurst, Edward G. McIver, John G. Moffat, Haitao Zhu, Anthony A. Estrada

PII: S0960-894X(18)30807-2
DOI: <https://doi.org/10.1016/j.bmcl.2018.10.017>
Reference: BMCL 26076

To appear in: *Bioorganic & Medicinal Chemistry Letters*

Received Date: 16 August 2018
Revised Date: 8 October 2018
Accepted Date: 12 October 2018

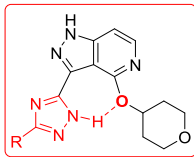
Please cite this article as: Shore, D.G.M., Sweeney, Z.K., Beresford, A., Chan, B.K., Chen, H., Drummond, J., Gill, A., Kleinheinz, T., Liu, X., Medhurst, A.D., McIver, E.G., Moffat, J.G., Zhu, H., Estrada, A.A., Discovery of potent azaindazole leucine-rich repeat kinase 2 (LRRK2) inhibitors possessing a key intramolecular hydrogen bond — Part 2, *Bioorganic & Medicinal Chemistry Letters* (2018), doi: <https://doi.org/10.1016/j.bmcl.2018.10.017>

This is a PDF file of an unedited manuscript that has been accepted for publication. As a service to our customers we are providing this early version of the manuscript. The manuscript will undergo copyediting, typesetting, and review of the resulting proof before it is published in its final form. Please note that during the production process errors may be discovered which could affect the content, and all legal disclaimers that apply to the journal pertain.

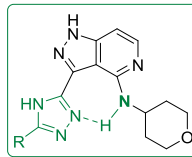


Discovery of potent azaindazole leucine-rich repeat kinase 2 (LRRK2) inhibitors possessing a key intramolecular hydrogen bond — Part 2

Daniel G. M. Shore, Zachary K. Sweeney, Alan Beresford, Bryan K. Chan, Huifen Chen, Jason Drummond, Andrew Gill, Tracy Kleinheinz, Xingrong Liu, Andrew D. Medhurst, Edward G. McIver, John G. Moffat, Haitao Zhu, and Anthony A. Estrada



LRRK2 K_i = 4600 nM



LRRK2 K_i = 7.8 nM

ACCEPTED MANUSCRIPT

Discovery of potent azaindazole leucine-rich repeat kinase 2 (LRRK2) inhibitors possessing a key intramolecular hydrogen bond — Part 2

Daniel G. M. Shore ^{a,1}, Zachary K. Sweeney ^{a,2}, Alan Beresford ^b, Bryan K. Chan ^a, Huifen Chen ^a, Jason Drummond ^c, Andrew Gill ^d, Tracy Kleinheinz ^c, Xingrong Liu ^e, Andrew D. Medhurst ^d, Edward G. McIver ^f,
John G. Moffat ^c, Haitao Zhu ^g, and Anthony A. Estrada ^{a,†}

^a Department of Discovery Chemistry, Genentech, Inc., 1 DNA Way, South San Francisco, CA 94080, USA

^b Department of Drug Metabolism and Pharmacokinetics, BioFocus, Chesterford Research Park, Saffron
Walden, Essex CB10 1XL, UK

^c Department of Biochemical and Cellular Pharmacology, Genentech, Inc., 1 DNA Way, South San Francisco,
CA 94080, USA

^d Department of Biochemical and Cellular Pharmacology, BioFocus, Chesterford Research Park, Saffron
Walden, Essex CB10 1XL, UK

^e Department of Drug Metabolism and Pharmacokinetics, Genentech, Inc., 1 DNA Way, South San Francisco,
CA 94080, USA

^f LifeArc, Accelerator Building, Open Innovation Campus, Stevenage SG1 2FX, UK

^g Department of Neuroscience, Genentech, Inc., 1 DNA Way, South San Francisco, CA 94080, USA

RECEIVED DATE

Abstract: The discovery of disease-modifying therapies for Parkinson's Disease (PD) represents a critical need in neurodegenerative medicine. Genetic mutations in LRRK2 are risk factors for the development of PD, and some of these mutations have been linked to increased LRRK2 kinase activity and neuronal toxicity in cellular and animal models. As such, research towards brain-permeable kinase inhibitors of LRRK2 has received much attention. In the course of a program to identify structurally diverse inhibitors of LRRK2

kinase activity, a 5-azaindazole series was optimized for potency, metabolic stability and brain penetration. A key design element involved the incorporation of an intramolecular hydrogen bond to increase permeability and potency against LRRK2. This communication will outline the structure-activity relationships of this matched pair series including the challenge of obtaining a desirable balance between metabolic stability and brain penetration.

Keywords: LRRK2; Kinase inhibitor; Azaindazole; Parkinson's disease; Brain penetration

ACCEPTED MANUSCRIPT

Mutations in the LRRK2 gene were first linked to familial Parkinson's disease (PD) more than a decade ago.[1] The most prevalent of these missense mutations, G2019S, has been shown to increase LRRK2 kinase activity in both biochemical and cellular assays.[2] Additionally, LRRK2 mutation carriers possess phenotypes that are indistinguishable from idiopathic PD.[3] Consequently, many research groups are pursuing LRRK2 kinase inhibitors as potential disease-modifying or neuroprotective therapies for both familial and sporadic cases of PD.[4][5]

Our group previously reported the discovery of highly potent, selective, and brain-penetrant LRRK2 small molecule inhibitors such as anilino-aminopyrimidine **GNE-7915 (1)**^d and aminopyrazole **GNE-0877 (2)**^f (Figure 1). These highly optimized compounds were evaluated in preclinical efficacy and safety studies to assess the consequences of prolonged in vivo LRRK2 kinase inhibition. In this communication, we describe the identification of structurally differentiated azaindazole LRRK2 inhibitors,[6] and highlight the use of intramolecular hydrogen bonding in the optimization of LRRK2 binding affinity. We also discuss the challenges associated with achieving in vivo brain penetration with the azaindazole N-H hinge-binding motif, and our attempts to improve membrane permeability through incorporation of intramolecular hydrogen bonding.[7]

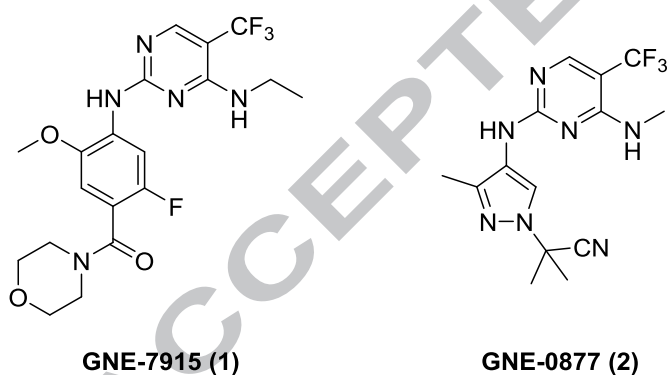
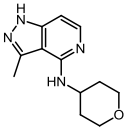
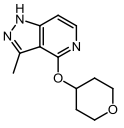
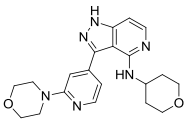
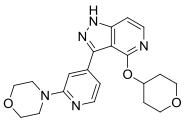


Figure 1. Previously described aminopyrimidine-based LRRK2 inhibitors

Profiles of azaindazole LRRK2 inhibitors, obtained from LifeArc (formerly MRC Technology), are shown in Table 1.^b[8] Small molecule inhibitors **3** and **4** were extensively profiled at Genentech and were confirmed to have good biochemical LRRK2 potency (182 nM and 44 nM, respectively). As such, they represented efficient starting points (**3**: LE = 0.56, LLE = 5.3, LELP = 2.7; **4**: LE = 0.61, LLE = 5.4, LELP = 3.1)[9][10] requiring kinase selectivity[11] and LRRK2 cellular potency optimization. DMPK

profiling of azaindazoles **3** and **4** demonstrated reasonable in vitro and in vivo metabolic stability and no P-gp-mediated efflux as measured by a MDCK-MDR1 assay (NIH cell line) using a compound concentration of 5 μ M. We also knew from inherited SAR that 4-alkoxy-substituted azaindazole inhibitors such as **4** were several fold more potent than the corresponding 4-amino analogues, (*cf.* compound **3**).**Error! Bookmark not defined.**^b

Table 1. MRCT azaindazole profiles

Cmpd	Structure	cLogP, TPSA ^a	LRRK2 Ki ^b (nM)	pLRRK2 ^c IC ₅₀ (nM)	LM Cl _{hep} (mL min ⁻¹ kg ⁻¹) ^d human / rat	MDR1 ^e P-gp ER ^f (B-A/A-B) ^g	Rat Cl (mL min ⁻¹ kg ⁻¹) ^h
3		1.5, 62	182	426	5.5 / 19	1.1	25
4		1.7, 60	44	301	6.0 / 21	0.9	34
5		2.1, 88	27	135	9.2 / 35	1.5	117
6		2.5, 85	4.2	24	14 / 49	3.4	69

^aTopological polar surface area

^bBiochemical assay

^cCellular assay; all biochemical and cellular assay results represent the arithmetic mean of a minimum of two determinations, and these assays generally produced results within 3-fold of the reported mean

^dLiver microsome predicted hepatic clearance

^eMDCK-MDR1 human P-gp transfected cell line

^fEfflux ratio

^gBasolateral-to-apical/apical-to-basolateral

^hCompounds dosed IV (1 mg/kg or 0.5 mg/kg) as a 40-60% PEG400 solution in H₂O

With a goal to increase the potency and kinase selectivity of this series, we turned to a LRRK2 homology model that has been previously described by our group.**Error! Bookmark not defined.**^c Figure 2a shows the proposed binding mode of **4** in the ATP binding site of LRRK2 overlaid with **GNE-7915 (1)**. Previous studies have shown that the front pocket region of the LRRK2 binding site, occupied by a phenyl ring in **1**, is a shallow and hydrophobic pocket optimally suited for flat aryl or heteroaryl rings. Appropriate substitution of the front pocket ring (methoxy substituent in **1**) typically yields high levels of kinase selectivity due to an invoked steric clash with residues such as Phe or Tyr (*cf.* Y931 of JAK2), which exist in

approximately 300 kinases.**Error! Bookmark not defined.**^c The modeled overlay (Figure 2a) supports our hypothesis that the modest kinase selectivity of **4** is due to the lack of an offensive interaction with Y931 of JAK2 (L1949 in LRRK2). We hypothesized that increased LRRK2 potency and selectivity of **4** versus off-target kinases, such as JAK2, would be improved with substituted 5- and 6-membered heteroaryl rings at the 3-position of the indazole. Figure 2b illustrates the proposed clash between 3-(2-morpholinopyridine) **6** and Y931 (yellow) of JAK2.

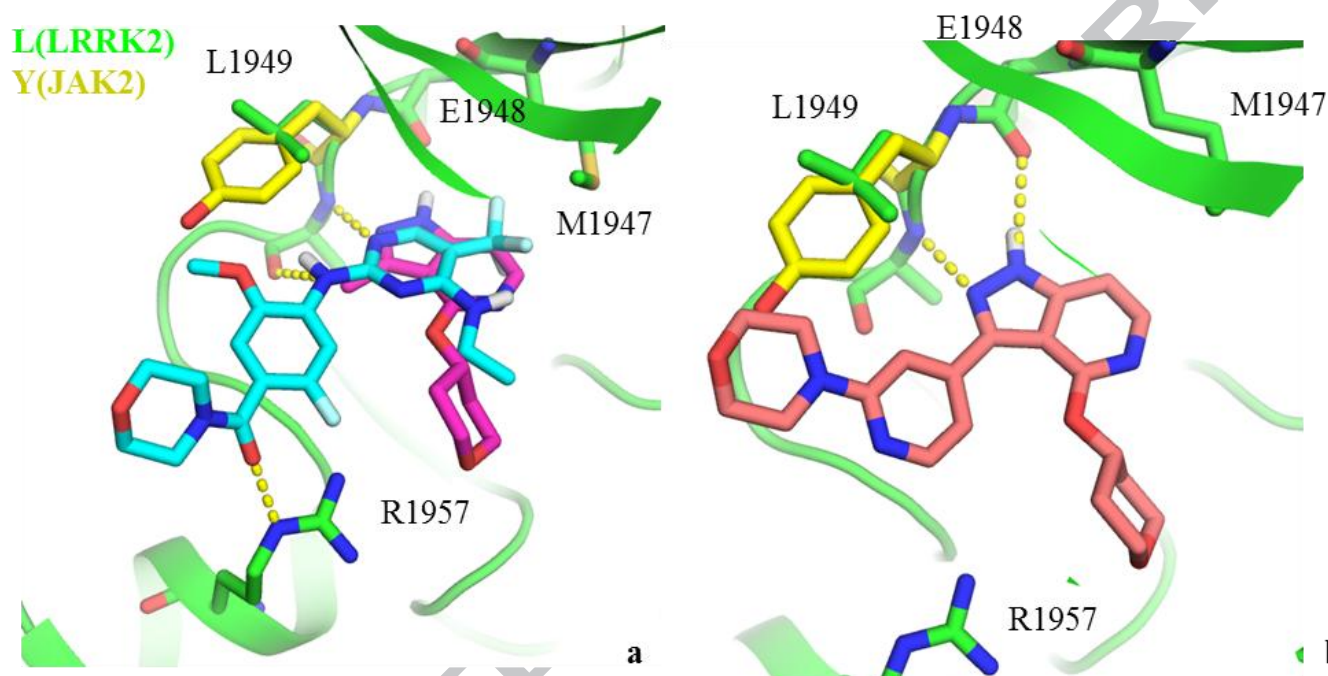


Figure 2. a) Overlay of docking models of **GNE-7915** (**1**) (cyan) and **4** (magenta) in the ATP binding site of a LRRK2 homology model with LRRK2 binding site residues (green) and Y931 of JAK2 (yellow). Predicted intermolecular hydrogen bonds are shown as yellow dashed lines. b) Predicted binding mode of **6** (salmon) in the ATP binding site of a LRRK2 homology model with LRRK2 binding site residues (green) and Y931 of JAK2 (yellow). Predicted intermolecular hydrogen bonds are shown as yellow dashed lines.

Morpholino substituted LifeArc compounds **5** and **6** with appropriately substituted 6-membered heteroaryl rings in the front pocket region are indeed potent and selective LRRK2 inhibitors (Table 1).**Error! Bookmark not defined.**^b Compound **6** demonstrates a JAK2/LRRK2 biochemical selectivity index of 882x and in a representative panel of 70 kinases at 1 μ M (237-fold over LRRK2 Ki), **6** only inhibited 2 off-target kinases at greater than 50% inhibition (MELK at 60% and TTK at 86%). The greater potency of **6** compared to **5** reproduces the previous observation that 4-alkoxyazaindazoles are generally more potent than the corresponding 4-aminoazaindazoles, possibly because the N-H of **5** causes the 3-aryl ring to be rotated slightly out of plane. Unfortunately, inhibitor **6** was cleared greater than liver blood flow in rat and appeared to be a modest P-gp substrate. Examination of the overall profiles for azaindoles **5** and **6** suggested that cLogP and

TPSA would need to be carefully modulated to appropriately balance metabolic stability and brain permeability.

Initial efforts focused on preparing close-in analogs of 4-alkoxyazaindazole **6** with 5- and 6-membered front pocket heterocycles (**7–10**, Table 2) engineered with increasing polarity compared to the more lipophilic compound **6**. Compound **7**, isomeric to **6** showed a marked decrease in potency with no improvement in metabolic stability. While an increase in metabolic stability was achieved with pyrazole **8**, the accompanying efflux ratio was unacceptable for sufficient brain penetration. Unsubstituted pyrazole **9** showed modest potency, possibly due to a co-planar confirmation encouraged by intramolecular hydrogen bonding between the pyrazole N-H and the alkoxy oxygen. Interestingly, 1,2,4-triazole **10** showed a sharp reduction in potency compared to pyrazoles **8** and **9**.

Table 2. 3-Heteroaryl substituted 5-azaindazoles

Cmpd	Structure	cLogP, TPSA ^a	LRRK2 K _i ^b (nM)	pLRRK2 ^c IC ₅₀ (nM)	LM Cl _{hep} (mL min ⁻¹ kg ⁻¹) ^d human / rat	MDR1 ^e P-gp ER ^f (B-A/A-B) ^g	Rat Cl (mL min ⁻¹ kg ⁻¹) ^h
7		2.7, 85	147	n.d. ⁱ	14 / 48	n.d. ⁱ	n.d. ⁱ
8		1.9, 98	21	13	2.0 / 22	80	30
9		2.1, 88	44	n.d. ⁱ	10 / 14	n.d. ⁱ	n.d. ⁱ
10		2.5, 101	4600	n.d. ⁱ	5.1 / 8.9	n.d. ⁱ	n.d. ⁱ

^aTopological polar surface area^bBiochemical assay^cCellular assay; all biochemical and cellular assay results represent the arithmetic mean of a minimum of two determinations, and these assays generally produced results within 3-fold of the reported mean^dLiver microsome predicted hepatic clearance^eMDCK-MDR1 human P-gp transfected cell line^fEfflux ratio^gBasolateral-to-apical/apical-to-basolateral^hCompounds dosed IV (0.5 mg/kg) as a 40-80% PEG400 solution in H₂O or 50-60% NMP solution in H₂OⁱNot determined

Quantum mechanical torsional scans[12] suggest that the dominant low-energy conformation of compound **10** is that shown in Figure 3 with a potential intramolecular hydrogen bond between the ether oxygen and the triazole N-H, and this conformation should be well accommodated in the flat front pocket binding site of LRRK2. However, this conformation of **10** also presents a lone pair towards a carbonyl oxygen on the protein backbone. We rationalized that the significant decrease in potency was due to disfavoured lone pair repulsion between a nitrogen on the 1,3,4-triazole moiety and a carbonyl oxygen on the protein backbone. This hypothesis also explains the diminished potency of compound **7** due to a similar disfavoured lone pair repulsion with the protein backbone.

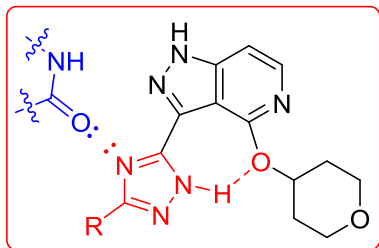


Figure 3. Lowest energy conformation of compound **8** with postulated intramolecular hydrogen bond and proposed repulsion with protein backbone

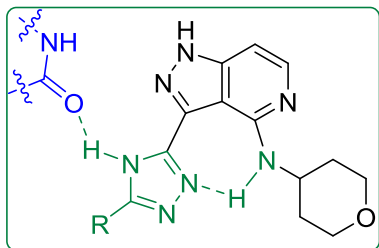


Figure 4. 4-aminoazaindazole is postulated to preserve the intramolecular hydrogen bond with a front pocket triazole while presenting an N-H to form putative favourable interactions with the protein backbone

Using this hypothesis, we postulated that a compound without this disfavoured interaction between the protein backbone and the inhibitor could result in improved potency. An intramolecular hydrogen bond between a nitrogen of the depicted triazole and the polar N-H of a 4-aminoazaindazole (Figure 4) could serve to favour the preferred flat conformation as well as provide a potential point of interaction between the inhibitor and the protein backbone through the triazole N-H. This could serve to rescue the potency of the 4-aminoazaindazole series compounds which were typically less potent than their 4-alkoxyazaindazole matched molecular pairs as shown in Table 1. In addition, the invoked intramolecular hydrogen bonding should mask the polarity, effectively neutralizing one hydrogen bond donor and acceptor, such that intrinsic permeability is improved and P-gp efflux may be reduced. **Error! Bookmark not defined.**[13]

3-heterocyclic-4-amino-5-azaindazoles which were capable of making an intramolecular hydrogen bond were designed and synthesized. Gratifyingly, compound **11** (Table 3) showed excellent biochemical (7.8 nM) and cellular potency (35 nM) representing a biochemical potency gain of 600-fold compared to the direct ether matched molecular pair **10**. Triazole **11** also demonstrated good in vitro microsomal stability and a moderate in vivo rat clearance of 36 mL min⁻¹ kg⁻¹. However, despite the masked polarity, compound **11** suffered from P-gp efflux (MDR1-MDCK efflux ratio of 21).

In an attempt to alleviate permeability concerns, several approaches were applied to decrease the polarity of the series. Compounds **12–17** (Table 3) exemplify employed strategies including the removal of

hydrogen bond donors and the reduction of polar surface area. It should be noted that substituting at the azaindazole N-H was not an option as this was a key hinge-binding element. Methylating the free N-H of the 1,3,4-triazole (**12**), resulted in an expected significant potency loss, likely due to steric clash with the protein backbone. Removal of one hydrogen bond donor through substitution with a 1,2,3-triazole (**13**) maintained desirable potency suggesting a C-H can potentially mimic the proposed interaction between the N-H of the triazole in **11** and the protein in some cases. However, P-gp mediated efflux was still significant. Pyrazoles **14** and **15**, with TPSA values of 80 and 71 respectively, demonstrated high levels of LRRK2 potency. However MDR1 efflux ratios were still unacceptable for brain penetration. Additionally, as polarity was reduced in an attempt to decrease MDR1 efflux, liver microsome stability predictably worsened (e.g. human LM Cl = 19 mL min⁻¹ kg⁻¹ for pyrazole **15**). This exemplifies the crucial balance that exists with this azaindazole series between permeability and stability. Notably, when regioisomeric pyrazole **16** was synthesized, potency was greatly reduced. This result serves as more evidence to the requirement of an intramolecular hydrogen bond for excellent LRRK2 potency using the 4-aminoazaindazole core since clearly no intramolecular hydrogen bonding can occur with this compound and significant out of plane torsion of the front pocket pyrazole is likely.

Table 3. 3-Heteroaryl substituted 4-amino-5-azaindazoles

Cmpd	Structure	cLogP, TPSA ^a	LRRK2 K _i ^b (nM)	pLRRK2 ^c IC ₅₀ (nM)	LM Cl _{hep} (mL min ⁻¹ kg ⁻¹) ^d human / rat	MDR1 ^e P-gp ER ^f (B-A/A-B) ^g	Rat Cl (mL min ⁻¹ kg ⁻¹) ^h
11		1.6, 104	7.8	35	7.0 / 11	21	35
12		1.4, 84	151	n.d. ⁱ	17 / 42	n.d. ⁱ	n.d. ⁱ
13		1.4, 93	1.2	49	10 / 31	23	n.d. ⁱ
14		2.2, 80	0.5	4.5	15 / 29	10	n.d. ⁱ
15		2.7, 71	3.5	n.d. ⁱ	19 / 47	4	n.d. ⁱ
16		2.1, 80	3900	n.d. ⁱ	10 / 29	11	n.d. ⁱ
17		2.0, 75	3.1	41	15 / 27	3.6	22
18		2.1, 88	4.1	24	13 / 23	1.4	18

^aTopological polar surface area^bBiochemical assay^cCellular assay; all biochemical and cellular assay results represent the arithmetic mean of a minimum of two determinations, and these assays generally produced results within 3-fold of the reported mean^dLiver microsome predicted hepatic clearance^eMDCK-MDR1 human P-gp transfected cell line^fEfflux ratio^gBasolateral-to-apical/apical-to-basolateral^hCompounds dosed IV (0.5 mg/kg) as a 40-80% PEG400 solution in H₂O or 50-60% NMP solution in H₂OⁱNot determined

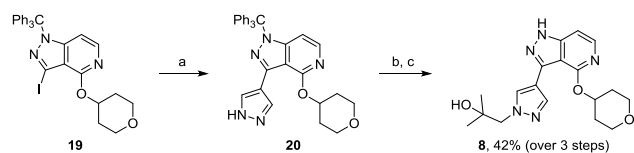
As we were unable to successfully incorporate the desired balance of potency, metabolic stability, and brain permeability with 4-aminoazaindazoles with 5-membered ring front-pocket heterocycles, 6-membered heterocycles capable of intramolecular hydrogen bonding were also synthesized. Compound **17** with a front-pocket pyridine was found to have excellent potency, although a modest P-gp liability still existed.

Trifluoropyrimidine **18** possessed excellent biochemical and cellular potency, in vitro stability, and lacked MDR1 efflux. Compounds **17** and **18** show considerably improved potency over compound **5** (Table 1), (which cannot participate in intramolecular hydrogen bonding,) and also greatly improved in vivo metabolic stability. Excellent selectivity of **18** was observed against JAK2 (1000-fold) as well as against the broader kinome, inhibiting only three other kinases at >50% at 1 μ M in a 74-kinase panel.[14] When **18** was analyzed in vivo, it distinguished itself from other azaindazoles by demonstrating moderate rat clearance ($18 \text{ mL}\cdot\text{min}^{-1} \text{ kg}^{-1}$),[15] good rat oral bioavailability (62 %),[16] and total and unbound brain to plasma ratios of 1.0 and 0.22 respectively.[17]

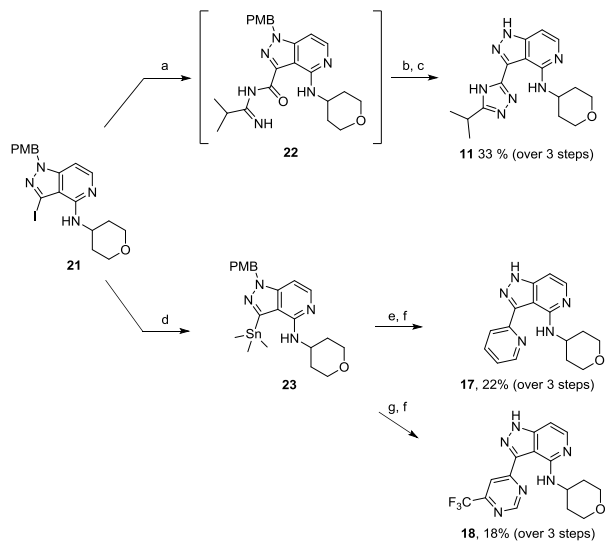
Compounds **8**, **10–18** were synthesized as described in Schemes 1–3.[18] Tertiary alcohol **8** was synthesized via a Suzuki reaction with 4-pyrazole boronic acid pinacol ester followed by alkylation with isobutylene oxide under basic conditions and deprotection of the trityl group with TFA and triethylsilane in dichloromethane. 1,3,4-triazoles **10–12** were synthesized starting from the appropriate PMB-protected 3-iodoazaindazole using a two-step, one-pot protocol involving a carbonylative C-N coupling with isopropyl amidine forming intermediate **22** followed by condensation of hydrazine[19] and subsequent PMB deprotection with triflic acid. Pyridine **17** and trifluoropyrimidine **18** were synthesized from the same starting material via a palladium-catalyzed stannylation to form stannane **23** followed by a Stille coupling and acidic PMB-deprotection.

1,2,3-triazole **13** was synthesized through a four-step sequence starting from the appropriate 1-trityl-protected azaindazole. A Sonogashira reaction with TMS-acetylene followed by methanolysis yielded the terminal alkyne **25**. A 1,3-dipolar cycloaddition of this terminal alkyne with sodium azide and in situ alkylation yielded the desired 1-isopropyl-1,2,3-triazole as a single regioisomer, which was converted to the final product through acidic trityl-deprotection. Pyrazole **14** was synthesized from the same trityl-protected azaindazole and pyrazole **15** was synthesized analogously. A Heck reaction with ethyl vinyl ketone yielded the α,β -unsaturated ketone **26**. This was condensed with hydrazine under microwave heating and oxidized with DDQ to give the N-H pyrazole, which was methylated and deprotected to give the final compound. It should be noted that methylation occurs selectively at the desired position, suggesting that the other pyrazole nitrogen is unavailable for alkylation due to intramolecular hydrogen-bonding. Lastly, to synthesize weakly potent

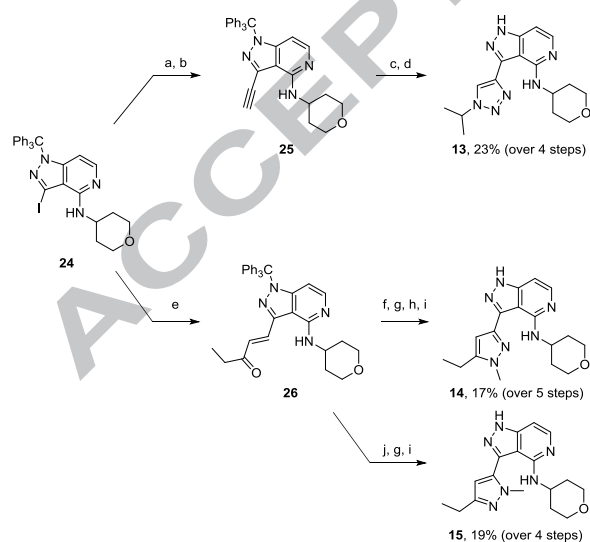
pyrazole isomer **16**, α,β -unsaturated ketone **26** was cyclized with methyl hydrazine under microwave heating, oxidized and deprotected as per pyrazole **14**.



Scheme 1. Reagents and conditions: (a) Pd(AmPhos)₂Cl₂, 4-pyrazole boronic acid pinacol ester, KOAc, Na₂CO₃, CH₃CN/H₂O, 150 °C, 90 min. (b) Isobutylene oxide, Cs₂CO₃, DMF, 80 °C, 2 h. (c) TFA, Et₃SiH, DCM, rt, 2 h.



Scheme 2. Reagents and conditions: (a) Isopropylamide hydrochloride, Pd(OAc)₂, XantPhos, Et₃N, CO atm, DMF, 80 °C, 2 h. (b) Hydrazine hydrate, HOAc, rt, 1 h. (c) TFOH, DCM, rt, 15 min. (d) Hexamethylditin, Pd(dppf)Cl₂, PhMe, 140 °C, 30 min. (e) 2-bromopyridine, Pd(PPh₃)₄, CuI, LiCl, THF, 100 °C, 30 min. (f) TFA, DCM, 150 °C, 2.5 h. (g) 4-bromo-6-trifluoromethylpyrimidine, Pd(PPh₃)₄, CuI, LiCl, THF, 100 °C, 30 min.



Scheme 3. Reagents and conditions: (a) TMSCH, Pd(PPh₃)₂Cl₂, CuI, Et₃N, CH₃CN, rt, 2 h. (b) K₂CO₃, MeOH, rt, 1 h. (c) Isopropyl iodide, NaN₃, CuI, 5:1 H₂O : 'BuOH, 100 °C, 16 h. (d) TFA, Et₃SiH, DCM, rt, 15 min. (e) Ethyl vinyl ketone, Pd(P(*o*-tol)₃)₂Cl₂, 'Pr₂NEt, DMF, 90 °C, 3 h. (f) Hydrazine hydrate, DMF, 180 °C, 10 min. (g) DDQ, DCM, rt, 16 h. (h) Cs₂CO₃, MeI, DMF, 60 °C, 2 h. (i) TFA, Et₃SiH, DCM, rt, 15 min. (j) Methyl hydrazine, DMF, 180 °C, 10 min.

In conclusion, we have presented a series of potent 3-heteroaryl-4-amino-5-azaindazole-based LRRK2 inhibitors. Optimal LRRK2 potency was contingent on the ability to invoke an intramolecular hydrogen bond between the 3-heteroaryl and 4-amino groups forming a 7-membered ring with no steric or electronic repulsion near the protein backbone. Though the balance of brain penetration and metabolic stability was a challenge within the hinge-binding azaindazole series, trifluoropyrimidine **18** showed excellent potency, and moderate in vivo rat clearance and brain penetration. Inhibitor **18** should contribute to the growing diversity of reported LRRK2 in vivo tool compounds and assist with exploring the diverse and emerging roles of LRRK2 function in preclinical studies.

Acknowledgements

The authors thank our Analytical, Bioanalytical, NMR, DMPK, Biochemical Pharmacology and Safety Assessment colleagues for their contributions.

Supplementary material

Supplementary data associated with this article can be found, in the online version, at <http://xxxx>

References and notes

References

- [1] (a) Zimprich, A.; Biskup, S.; Leitner, P.; Lichtner, P.; Farrer, M.; Lincoln, S.; Kachergus, J.; Hulihan, M.; Uitti, R. J.; Calne, D.B.; Stoessl, A. J.; Pfeiffer, R. F.; Patenge, N.; Carbajal, I. C.; Vieregge, P.; Asmus, F.; Muller-Myhsok, B.; Dickson, D. W.; Meitinger, T.; Strom, T. M.; Wszolek, Z. K.; Gasser, T. *Neuron* **2004**, *44*, 601; (b) Haslam, E. *Shikimic Acid Metabolism and Metabolites*, John Wiley & Sons: New York, 1993; (c) Paisan-Ruiz, C.; Jain, S.; Evans, E. W.; Gilks, W. P.; Simon, J.; van der Brug, M.; Lopez de Munain, A.; Aparicio, S.; Gil, A. M.; Khan, N.; Johnson, J.; Martinez, J. R.; Nicholl, D.; Carrera, I. M.; Pena, A. S.; de Silva, R.; Lees, A.; Marti-Masso, J. F.; Perez-Tur, J.; Wood, N. W.; Singleton, A. B. *Neuron* **2004**, *44*, 595; (d) Lees, A. J.; Hardy, J.; Revesz, T. Parkinson's disease. *Lancet* **2009**, *373*, 2055. Erratum in: *Lancet* **2009**, *374*, 684.

[2] (a) West, A. B.; Moore, D. J.; Biskup, S.; Bugayenko, A.; Smith, W. W.; Ross, C. A.; Dawson, V. L.; Dawson, T. M. *Proc. Natl. Acad. Sci. USA* **2005**, *102*, 16842; (b) Greggio, E.; Jain, S.; Kingsbury, A.; Bandopadhyay, R.; Lewis, P.; Kaganovich, A.; van der Brug, M. P.; Beilina, A.; Blackinton, J.; Thomas, K. J.; Ahmad, R.; Miller, D. W.; Kesavapany, S.; Singleton, A.; Lees, A.; Harvey, R. J.; Harvey, K.; Cookson, M. R. *Neurobiol. Dis.* **2006**, *23*, 329; (c) Cookson, M. R. *Nat. Rev. Neurosci.* **2010**, *11*, 791; (d) Liu, Z.; Hamamichi, S.; Lee, B. D.; Yang, D.; Ray, A.; Caldwell, G. A.; Caldwell, K. A.; Dawson, T. M.; Smith, W. W.; Dawson, V. L. *Hum. Mol. Genet.* **2011**, *20*, 3933; (e) Lee, B. D.; Shin, J-H.; VanKampen, J.; Petrucelli, L.; West, A. B.; Ko, H. S.; Lee, Y-I.; Maguire-Zeiss, K. A.; Bowers, W. J.; Federoff, H. J.; Dawson, V. L.; Dawson, T. M. *Nat. Med.* **2010**, *16*, 998; (f) Lee, B. D.; Dawson, V. L.; Dawson, T. M. *Trends in Pharmacol. Sci* **2012**, *33*, 365; (g) Ramsden, N.; Perrin, J.; Ren, Z.; Lee, B. D.; Zinn, N.; Dawson, V. L.; Tam, D.; Bova, M.; Lang, M.; Drewes, G.; Bantscheff, M.; Bard, F.; Dawson, T. M.; Hopf, C. *ACS Chem. Biol.* **2011**, *6*, 1021; (h) Smith, W. W.; Pei, Z.; Jiang, H.; Dawson, V. L.; Dawson, T. M.; Ross, C. A. *Nat. Neurosci.* **2006**, *9*, 1231; (i) MacLeod, D.; Dowman, J.; Hammond, R.; Leete, T.; Inoue, K.; Abeliovich, A. *Neuron* **2006**, *52*, 587.

[3] (a) Marras, C.; Schüle, B.; Munhoz, R. P.; Rogaeva, E.; Langston, J. W.; Kasten, M.; Meaney, C.; Klein, C.; Wadia, P. M.; Lim, S. Y.; Chuang, R. S.; Zadikof, C.; Steeves, T.; Prakash, K. M.; de Bie, R. M.; Adeli, G.; Thomsen, T.; Johansen, K. K.; Teive, H. A.; Asante, A.; Reginold, W.; Lang, A. E. *Neurology* **2011**, *77*, 325; (b) Dachsel, J. C.; Farrer, M. J. *Arch. Neurol.* **2010**, *67*, 542; (c) Satake, W.; Nakabayashi, Y.; Mizuta, I.; Hirota, Y.; Ito, C.; Kubo, M.; Kawaguchi, T.; Tsunoda, T.; Watanabe, M.; Takeda, A.; Tomiyama, H.; Nakashima, K.; Hasegawa, K.; Obata, F.; Yoshikawa, T.; Kawakami, H.; Sakoda, S.; Yamamoto, M.; Hattori, N.; Murata, M.; Nakamura, Y.; Toda, T. *Nat. Genet.* **2009**, *41*, 1303; (d) Simón-Sánchez, J.; Schulte, C.; Bras, J. M.; Sharma, M.; Gibbs, J. R.; Berg, D.; Paisan-Ruiz, C.; Lichtner, P.; Scholz, S. W.; Hernandez, D. G.; Krüger, R.; Federoff, M.; Klein, C.; Goate, A.; Perlmutter, J.; Bonin, M.; Nalls, M.A.; Illig, T.; Gieger, C.; Houlden, H.; Steffens, M.; Okun, M. S.; Racette, B. A.; Cookson, M.R.; Foote, K. D.; Fernandez, H. H.; Traynor, B. J.; Schreiber, S.; Arepalli, S.; Zonozi, R.; Gwinn, K.; van der Brug, M.; Lopez, G.; Chanock, S. J.; Schatzkin, A.; Park, Y.; Hollenbeck, A.; Gao, J.; Huang, X.; Wood, N. W.; Lorenz, D.; Deuschl, G.; Chen, H.; Riess, O.; Hardy, J. A.; Singleton, A. B.; Gasser, T. *Nat. Genet.* **2009**, *41*, 1308.

[4] (a) Deng, X.; Dzamko, N.; Prescott, A.; Davies, P.; Liu, Q.; Yang, Q.; Lee, J-D.; Patricelli, M. P.; Nomanbhoy, T. K.; Alessi, D. R.; Gray, N. S. *Nat. Chem. Bio.* **2011**, *7*, 203; (b) Zhang, J.; Deng, X.; Choi, H. G.; Alessi, D. R.; Gray, N. S. *Bioorg. Med. Chem. Lett.* **2012**, *22*, 1864; (c) Chen, H.; Chan, B. K.; Drummond, J.; Estrada, A. A.; Gunzner-Toste, J.; Liu, X.; Liu, Y.; Moffat, J. G.; Shore, D.; Sweeney, Z. K.; Tran, T.; Wang, S.; Zhao, G.; Zhu, H.; Burdick, D. J. *J. Med. Chem.* **2012**, *55*, 5536; (d) Estrada, A. A.; Liu, X.; Baker-Glenn, C.; Beresford, A.; Burdick, D. J.; Chambers, M.; Chan, B. K.; Chen, H.; Ding, X.; DiPasquale, A. G.; Dominguez, S. L.; Dotson, J.; Drummond, J.; Flagella, M.; Flynn, S.; Fuji, R.; Gill, A.; Gunzner-Toste, J.; Harris, S. F.; Heffron, T. P.; Kleinheinz, T.; Lee, D. W.; Le Pichon, C. E.; Lyssikatos, J. P.; Medhurst, A. D.; Moffat, J. G.; Mukund, S.; Nash, K.; Scarce-Levie, K.; Sheng, Z.; Shore, D. G.; Tran, T.; Trivedi, N.; Wang, S.; Zhang, S.; Zhang, X.; Zhao, G.; Zhu, H.; Sweeney, Z. K. *J. Med. Chem.* **2012**, *55*, 9416; (e) Chan, B. K.; Estrada, A. A.; Chen, H.; Atherall, J.; Baker-Glenn, C.; Beresford, A.; Burdick, D. J.; Chambers, M.; Dominguez, S. L.; Drummond, J.; Gill, A.; Kleinheinz, T.; Le Pichon, C. E.; Medhurst, A. D.; Liu, X.; Moffat, J. G.; Nash, K.; Scarce-Levie, K.; Sheng, Z.; Shore, D. G.; Van de Poël, H.; Zhang, S.; Zhu, H.; Sweeney, Z. K. *ACS Med. Chem. Lett.* **2013**, *4*, 85; (f) Estrada, A. A.; Chan, B. K.; Baker-Glenn, C.; Beresford, A.; Burdick, D. J.; Chambers, M.; Chen, H.; Dominguez, S. L.; Dotson, J.; Drummond, J.; Flagella, M.; Fuji, R.; Gill, A.; Halladay, J.; Harris, S. F.; Heffron, T. P.; Kleinheinz, T.; Lee, D. W.; Le Pichon, C. E.; Liu, X.; Lyssikatos, J. P.; Medhurst, A. D.; Moffat, J. G.; Nash, K.; Scarce-Levie, K.; Sheng, Z.; Shore, D. G.; Wong, S.; Zhang, S.; Zhang, X.; Zhu, H.; Sweeney, Z. K. *J. Med. Chem.* **2014**, *57*, 921; (g) Choi, H. G.; Zhang, J.; Deng, X.; Hatcher, J. M.; Patricelli, M. P.; Zhao, Z.; Alessi, D. R.; Gray, N. S. *ACS Med. Chem. Lett.* **2012**, *3*, 658; (h) Reith, A. D.; Bamborough, P.; Jandu, K.; Andreotti, D.; Mensah, L.; Dossang, P.; Choi, H. G.; Deng, X.; Zhang, J.; Alessi, D. R.; Gray, N. S. *Bioorg. Med. Chem. Lett.* **2012**, *22*, 5625; (i) Hermanson, S. B.; Carlson, C. B.; Riddle, S. M.; Zhao, J.; Vogel, K. W.; Nichols, R. J.; Bi, K. *PLoS One*, **2012**, *7*, e43580; (j) Franzini, M.; Ye, X. M.; Adler, M.; Aubele, D. L.; Garofalo, A. W.; Gauby, S.; Goldbach, E.; Probst, G. D.; Quinn, K. P.; Santiago, P.; Sham, H. L.; Tam, D.; Truong, A.; Ren, Z. *Bioorg. Med. Chem. Lett.* **2013**, *23*, 1967; (k) Garofalo, A. W.; Adler, M.; Aubele, D. L.; Brigham, E. F.; Chian, D.; Franzini, M.; Goldbach, E.; Kwong, G. T.; Motter, R.; Probst, G. D.; Quinn, K. P.; Ruslim, L.; Sham, H. L.; Tam, D.; Tanaka, P.; Truong, A. P.; Ye, X. M.; Ren, Z. *Bioorg. Med. Chem. Lett.* **2013**, *23*, 1974; (l) Liu, M.; Bender, S. A.; Cuny, G. D.;

Sherman, W.; Glicksman, M.; Ray, S. S. *Biochemistry* **2013**, *52*, 1725; (m) Liu, M.; Bender, S. A.; Cuny, G. D.; Sherman, W.; Glicksman, M.; Ray, S. S. *Biochemistry* **2013**, *52*, 1725; (n) Troxler, T.; Greenidge, P.; Zimmermann, K.; Desrayaud, S.; Druckes, P.; Schweizer, T.; Stauffer, D.; Rovelli, G.; Shimshek, D. R. *Bioorg. Med. Chem. Lett.* **2013**, *23*, 4085; (o) Feng, Y.; Chambers, J. W.; Iqbal, S.; Koenig, M.; Park, H.; Cherry, L.; Hernandez, P.; Figuera-Losada, M.; LoGrasso, P. V. *ACS Chem. Biol.* **2013**, *8*, 1747; (p) Galatsis, P.; Henderson, J. L.; Kormos, B. L.; Han, S.; Kurumbail, R. G.; Wager, T. T.; Verhoest, P. R.; Noel, G. S.; Chen, Y.; Needle, E.; Berger, Z.; Steyn, S. J.; Houle, C.; Hirst, W. *Bioorg. Med. Chem. Lett.* **2014**, *24*, 4132; (q) Fell, M. J.; Mirescu, C.; Basu, K.; Cheewatrakoolpong, B.; DeMong, D. E.; Ellis, J. M.; Hyde, L. A.; Lin, Y.; Markgraf, C. G.; Mei, H.; Miller, M.; Poulet, F. M.; Scott, J. D.; Smith, M. D.; Yin, Z.; Zhou, X.; Parker, E. M.; Kennedy, M. E.; Morrow, J. A. *J. Pharmacol. Exp. Ther.* **2015**, *355*, 397; (r) Galatsis, P.; Hayward, M. M.; Kormos, B. L.; Wager, T. T.; Zhang, L.; Stepan, A. F.; Henderson, J. L.; Kurumbail, R. G.; Verhoest, P. R. US9642855B2, 2015; (s) Henderson, J. L.; Kormos, B. L.; Hayward, M. M.; Co, K. J.; Jasti, J.; Kurumbail, R. G.; Wager, T. T.; Verhoest, P. R.; Noell, G. S.; Chen, Y.; Needle, E.; Berger, Z.; Steyn, S. J.; Houle, C.; Hirst, W. D.; Galatsis, P. *J. Med. Chem.* **2015**, *58*, 419; (t) Scott, J. D.; DeMong, D. E.; Greshock, T. J.; Basu, K.; Dai, X.; Harris, J.; Hruza, A.; Li, S. W.; Lin, S.; Liu, H.; Macala, M. K.; Hu, Z.; Mei, H.; Zhang, H.; Walsh, P.; Poirier, M.; Shi, Z.; Xiao, L.; Agnihotri, G.; Baptista, M. A. S.; Columbus, J.; Fell, M. J.; Hyde, L. A.; Kuvelkar, R.; Lin, Y.; Mirescu, C.; Morrow, J. A.; Yin, Z.; Zhang, X.; Zhou, X.; Chang, R. K.; Embrey, M. W.; Sanders, J. M.; Tiscia, H. E.; Drolet, R. E.; Kern, J. T.; Sur, S. M.; Renger, J. J.; Bilodeau, M. T.; Kennedy, M. E.; Parker, E. M.; Stamford, A. W.; Nargund, R.; McCauley, J. A.; Miller, M. W. *J. Med. Chem.* **2017**, *60*, 2983.

[5] For recent reviews on LRRK2 small molecule kinase inhibitors, see: (a) Kramer, T.; Lo Monte, F.; Göring, S.; Amombo, G. M. O.; Schmidt, B. *ACS Chem. Neurosci.* **2012**, *3*, 151. (b) Kavanagh, M. E.; Doddareddy, M. R.; Kassiou, M. *Bioorg. Med. Chem. Lett.* **2013**, *23*, 3690. (c) Dzamko, N.; Halliday, G. M. *Future Neurol.* **2013**, *8*, 347; (d) Estrada, A. A.; Sweeney, Z. K. *J. Med. Chem.* **2015**, *58*, 6733; (e) Taymans, J.-M.; Greggio, E. *Curr. Neuropharmacol.* **2016**, *14*, 214; (f) Atashrazm, F.; Dzamko, N. *Clin. Pharmacol.* **2016**, *8*, 177; (g) West, A. B. *Exp. Neurol.* **2017**, *298*, 236; (h) Hatcher, J. M.; Choi, H. G.; Alessi, D. R.;

- Gray, N. S.; Rideout, H. (ed) *Adv. Neurobiol.* **2017**, *14*, 241; (i) Alessi, D. R.; Sammler, E. *Science* **2018**, 360, 36.
- [6] (a) Chan, B. K.; Chen, H.; Estrada, A.; Shore, D.; Sweeney, Z.; McIver, E. G. US8569281B2, 2013; (b) Osborne, J.; Birchall, K.; Harding, D. J.; Lewis, S. J.; Smiljanic-Hurley, E.; Taylor, D. L.; Levy, A.; Alessi, D.; McIver, E. G. *Bioorg. Med. Chem. Lett.* **2018**, *in press*.
- [7] (a) Kuhn, B.; Mohr, P.; Stahl, M. *J. Med. Chem.* **2010**, *53*, 2601; (b) Desai, P. V.; Raub, T. J.; Blanco, M.-J. *Bioorg. Med. Chem. Lett.* **2012**, *22*, 6540.
- [8] McIver, E. G.; Smiljanic, E.; Harding, D. J.; Hough, J. WO2010106333A1, 2010
- [9] LE: Ligand Efficiency; LLE: Ligand Lipophilic Efficiency; LELP: Ligand Efficiency-Dependent Lipophilicity. *Discov.* **2007**, *6*, 881; (c) Keserü, G. M.; Makara, G. M. *Nat. Rev. Drug Discov.* **2009**, *8*, 203.
- [10] (a) Hopkins, A. L.; Groom, C. R.; Alex, A. *Drug Discov. Today* **2004**, *9*, 430; (b) Leeson, P. D.; Springthorpe, B. *Nat. Rev. Drug*
- [11] JAK2 selectivity indices for **3** and **4** were 20-fold. JAK2 selectivity was used as a surrogate for general kinase selectivity, see ref. 4c.
- [12] (a) *Jaguar*, version 8.1; Schrödinger, LCC: New York, **2013**. (b) Bochevarov, A. D.; Harder, E.; Hughes, T. F.; Greenwood, J. R.; Braden, D. A.; Philipp, D. M.; Rinaldo, D.; Halls, M. D.; Zhang, J.; Friesner, R. A. *Int. J. Quantum Chem.* **2013**, *113*, 2110.
- [13] Rafi, S. B.; Hearn, B. R.; Vedantham, P.; Jacobsen, M. P.; Renslo, A. R. *J. Med. Chem.* **2012**, *55*, 3163.
- [14] Compound **16** at a compound concentration of 1 μ M inhibited MST4 at 59%, TAK1-TAB1 at 51% and TTK at 52%.
- [15] Compound **16** was dosed IV (0.5 mg/kg) as a 51% NMP solution in H₂O.
- [16] Compound **16** was dosed PO (1 mg/kg) as an aqueous suspension with 1% methylcellulose.
- [17] AUC ratio; compound **16** was dosed IV (0.5 mg/kg) as a 60% NMP solution in H₂O.

- [18] Compounds **5** and **6** were synthesized as described previously, see ref. **Error! Bookmark not defined.**
- [19] Staben, S. T.; Blaquiere, N. *Angew. Chem. Int. Ed.* **2010**, *49*, 325.

ACCEPTED MANUSCRIPT

Highlights

- A series of potent azaindazole inhibitors of LRRK2 was discovered
- A putative intramolecular hydrogen bond was crucial for LRRK2 potency of 4-aminoazaindazole compounds
- Careful optimization of polarity and conformation was necessary to ensure potency, metabolic stability and brain permeability
- Compound **18** showed excellent LRRK2 potency, and moderate in vivo rat clearance and brain penetration

ACCEPTED MANUSCRIPT